

# Lawrence Berkeley Laboratory

UNIVERSITY OF CALIFORNIA

To be presented at the Medical Imaging IV Conference,  
Newport Beach, CA, February 4-9, 1990, and  
to be published in the Proceedings

## Linear Analysis of Rotationally Invariant, Radially Variant Tomographic Imaging Systems

J.R. Baker, R.H. Huesman, and T.F. Budinger

January 1990

**For Reference**

**Not to be taken from this room**

# Donner Laboratory

# Biology & Medicine Division

## **DISCLAIMER**

This document was prepared as an account of work sponsored by the United States Government. While this document is believed to contain correct information, neither the United States Government nor any agency thereof, nor the Regents of the University of California, nor any of their employees, makes any warranty, express or implied, or assumes any legal responsibility for the accuracy, completeness, or usefulness of any information, apparatus, product, or process disclosed, or represents that its use would not infringe privately owned rights. Reference herein to any specific commercial product, process, or service by its trade name, trademark, manufacturer, or otherwise, does not necessarily constitute or imply its endorsement, recommendation, or favoring by the United States Government or any agency thereof, or the Regents of the University of California. The views and opinions of authors expressed herein do not necessarily state or reflect those of the United States Government or any agency thereof or the Regents of the University of California.

Linear Analysis of Rotationally Invariant, Radially  
Variant Tomographic Imaging Systems

J.R. Baker<sup>†\*</sup>, R.H. Huesman\*, and T.F. Budinger<sup>†\*</sup>

<sup>†</sup>Department of Electrical Engineering and Computer Sciences  
University of California

and

\*Research Medicine and Radiation Biophysics Division  
Lawrence Berkeley Laboratory  
University of California  
Berkeley, CA 94720

January 1990

This work was supported by the Office of Energy Research,  
Office of Health and Environmental Research, of the U. S. Department of  
Energy under Contract No. DE-AC03-76SF00098, by the National Institutes  
of Health, National Heart, Lung, and Blood Institute under grants No  
HL07367 and HL25840, National Institute of Aging under grant AG05890,  
by Cray Research Inc., and by IBM Inc.

# Linear analysis of rotationally invariant, radially variant tomographic imaging systems

John R. Baker<sup>†‡</sup>, Ronald H. Huesman<sup>†</sup>, and Thomas F. Budinger<sup>†‡</sup>

<sup>†</sup>Department of Electrical Engineering and Computer Sciences  
University of California, Berkeley

<sup>‡</sup>Research Medicine and Radiation Biophysics Division  
Lawrence Berkeley Laboratory  
University of California  
1 Cyclotron Road  
Berkeley, CA 94720

## ABSTRACT

We describe a method to analyze the linear imaging characteristics of rotationally invariant, radially variant tomographic imaging systems using singular value decomposition (SVD). When the projection measurements from such a system are assumed to be samples from independent and identically distributed multi-normal random variables, the best estimate of the emission intensity is given by the unweighted least squares estimator. The noise amplification of this estimator is inversely proportional to the singular values of the normal matrix used to model projection and backprojection. After choosing an acceptable noise amplification, the new method can determine the number of parameters and hence the number of pixels that should be estimated from data acquired from an existing system with a fixed number of angles and projection bins. Conversely, for the design of a new system, the number of angles and projection bins necessary for a given number of pixels and noise amplification can be determined. In general, computing the SVD of the projection normal matrix has cubic computational complexity. However, the projection normal matrix for this class of rotationally invariant, radially variant systems has a block circulant form. A fast parallel algorithm to compute the SVD of this block circulant matrix makes the singular value analysis practical by asymptotically reducing the computation complexity of the method by a multiplicative factor equal to the number of angles squared.

## 1 INTRODUCTION

Using singular value decomposition (SVD), the performance of an imaging system can be determined when the projection measurements are independent and identically distributed multi-normal random variables. The best estimate of the emission intensity is given by the unweighted least squares estimator.<sup>[1]</sup> This estimator can be obtained by applying the pseudo-inverse of the projection formation tensor to the measured projection data. The pseudo-inverse is easily computed from its SVD.<sup>[2]</sup> The noise amplification of the imaging system is inversely proportional to the square of the singular values of the projection formation tensor.

The computation of the singular value decomposition of the projection tensor, in general, has a cubic computational complexity. Thus, the use of this technique has traditionally been impractical for many systems.

### 1.1 Data acquisition

Projection formation can be described by the discrete-continuous model<sup>[3],[4]</sup>

$$p_{\theta k} = F_{\theta k} b \tag{1}$$

$$= \int dy \int dx f_{\theta k}(x, y) b(x, y) \tag{2}$$

where  $p_{\theta k}$  is the measured projection at angle index  $\theta$  and bin position  $k$ .  $F_{\theta k}$  is a second order tensor functional operating on the two dimensional object distribution  $b$ . This represents the integration of the product of the impulse response or transition probabilities  $f_{\theta k}(x, y)$  and the object distribution  $b(x, y)$  over the imaging field as depicted in figure 1. There are  $m_{\theta}$  different angles and  $m_k$  projection bins at each angle.

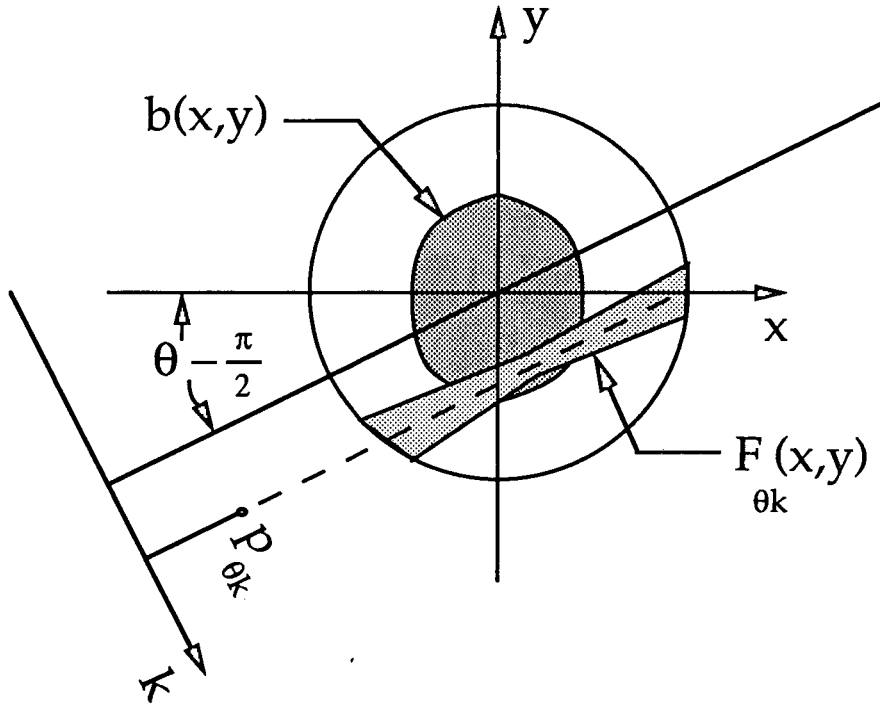


Figure 1: Schematic of projection formation.

Because the model assumes the detection process is discrete and the original distribution to be continuous, the model is easily adapted to include a variety of physical effects found in positron tomography, single photon emission computed tomography, nuclear magnetic resonance imaging, and other imaging modalities. For positron tomography,  $F_{\theta k}$  can include radioactive decay, positron range, sampling geometry, attenuation, inter-crystal scatter, crystal penetration, and detection efficiency.<sup>[5]</sup>

One simple but important statistic model of each acquired signal,  $p_{\theta k}$ , is to assume that it is a sample from an independent and identically distributed multi-normal random variable. The distribution is determined by the first two central moments, which are the mean

$$\mu_{p_{\theta k}} = E p_{\theta k} \quad (3)$$

$$= F_{\theta k} b \quad (4)$$

and covariance

$$\Sigma_{\theta' k' \theta k} = E [(p_{\theta' k'} - E p_{\theta' k'}) (p_{\theta k} - E p_{\theta k})] \quad (5)$$

$$= E [p_{\theta' k'} p_{\theta k}] - \mu_{\theta' k'} \mu_{\theta k} \quad (6)$$

$$= \bar{p} \delta_{\theta' \theta} \delta_{k' k} \quad (7)$$

where  $\bar{p}$  is a constant.

## 1.2 Estimation

The goal of tomography is to reconstruct the unknown distribution  $b$  from one realization,  $p_{\theta k}$  of the measurement process  $p_{\theta k}$ . Unfortunately, recovering the continuous distribution  $b$  is difficult, if not impossible. Instead, a discretized version,  $b_{ij}$ , shown in equation 8, is estimated from the measurements where  $B_{ij}$  define a generalized pixel. Thus,  $b_{ij}$  is the value  $(i, j)^{\text{th}}$  pixel assumes.

$$b(x, y) \approx b_{ij} B_{ij}(x, y) \quad (8)$$

In this basis, the projection formation equation becomes

$$\tilde{p}_{\theta k} = F_{\theta k} B_{ij} b_{ij} \quad (9)$$

$$= F_{\theta k ij} b_{ij} \quad (10)$$

where there is an implied sum over repeated subscripts, or rewritten in matrix-vector notation

$$\tilde{\mathbf{p}} = \mathbf{F} \mathbf{b}. \quad (11)$$

However, the choice of basis functional  $B_{ij}$  determines the systematic error which is defined as the difference between  $p_{\theta k}$  and  $\tilde{p}_{\theta k}$ . In this paper, we will assume that the errors have been minimized by the appropriate basis choice.<sup>[6]</sup>

With this choice of basis, the least squares estimator is given by equation 12.

$$\hat{\mathbf{b}} = \arg \min_{\mathbf{b}} E \left\{ (\underline{\mathbf{p}} - \mathbf{F} \mathbf{b})^T (\underline{\mathbf{p}} - \mathbf{F} \mathbf{b}) \right\} \quad (12)$$

$$= \arg \left\{ [\mathbf{F}^T (\underline{\mathbf{p}} - \mathbf{F} \mathbf{b})] = 0 \right\} \quad (13)$$

$$= (\mathbf{F}^T \mathbf{F})^{-1} \mathbf{F}^T \underline{\mathbf{p}} \quad (14)$$

$$= (\mathbf{V} \mathbf{S}^T \mathbf{U}^T \mathbf{U} \mathbf{S} \mathbf{V}^T)^{-1} \mathbf{V} \mathbf{S}^T \mathbf{U}^T \underline{\mathbf{p}} \quad (15)$$

$$= \mathbf{V} (\mathbf{S}^T \mathbf{S})^{-1} \mathbf{S}^T \mathbf{U}^T \underline{\mathbf{p}} \quad (16)$$

$$= \mathbf{F}^+ \underline{\mathbf{p}} \quad (17)$$

$\mathbf{F}^+$  is the pseudo-inverse of  $\mathbf{F}$  and is computed from the SVD

$$\mathbf{F} = \mathbf{U}\mathbf{S}\mathbf{V}^T \quad (18)$$

where  $\mathbf{U}$  and  $\mathbf{V}$  are matrices containing the left and right singular vectors of  $\mathbf{F}$ , respectively.  $\mathbf{S}$  is a generalized diagonal matrix containing the singular values of  $\mathbf{F}$ . The covariance matrix for the estimator is given by equation 19.

$$\Sigma_{\hat{\mathbf{b}}} = \text{Cov}(\hat{\mathbf{b}}) \quad (19)$$

$$= \mathbf{F}^+ \Sigma_{\mathbf{p}} (\mathbf{F}^+)^T \quad (20)$$

$$= \mathbf{F}^+ \bar{p} \mathbf{I} (\mathbf{F}^+)^T \quad (21)$$

$$= \bar{p} \mathbf{F}^+ (\mathbf{F}^+)^T \quad (22)$$

$$= \bar{p} \mathbf{V} (\mathbf{S}^T \mathbf{S})^{-1} \mathbf{V}^T \quad (23)$$

## 2 ANALYSIS

### 2.1 Error bound

To bound the statistical error associated with the reconstruction process, we compute the  $L_2$  norm of the covariance matrix using induced norms as shown in equation 24. When computing the induced norm, a unit vector  $\mathbf{b}$  is multiplied by the covariance matrix and the norm of the resulting vector is calculated. The length of the unit vector is scaled up or down and the square of the largest scale factor is the induced norm. From the induced norm, it can be seen that the noise amplification bound during reconstruction is inversely proportional to the square of the smallest singular value of the projection formation matrix. Thus, it is necessary to find the singular values of  $F$  to compute the error bound. This differs from the deterministic approach where the noise amplification is the ratio of the largest singular value to the smallest singular value; e.g., the condition number.<sup>[2]</sup>

$$\|\Sigma_{\hat{\mathbf{b}}}\|_2 = \max_{\|\mathbf{b}\|_2=1} \|\Sigma_{\hat{\mathbf{b}}}\mathbf{b}\|_2 \quad (24)$$

$$= \max_{\|\mathbf{b}\|_2=1} \|\bar{p}\mathbf{V} (\mathbf{S}^T \mathbf{S})^{-1} \mathbf{V}^T \mathbf{b}\|_2 \quad (25)$$

$$= \max_{\|\mathbf{b}\|_2=1} \bar{p} \|(\mathbf{S}^T \mathbf{S})^{-1} \mathbf{b}\|_2 \quad (26)$$

$$= \max \bar{p} \frac{1}{S_{ii}^2} \quad (27)$$

$$= \frac{\bar{p}}{\min S_{ii}^2} \quad (28)$$

### 2.2 Computation of singular values

The normal or self-adjoint matrix,  $\mathbf{A}$ , which backprojects  $p_{\theta k}$  and reprojects it to  $p_{\theta' k'}$  has elements

$$A_{\theta' k' \theta k} = F_{\theta' k'} F_{\theta k} \quad (29)$$

$$= \int dy \int dx f_{\theta' k'}(x, y) f_{\theta k}(x, y) \quad (30)$$

and represents overlap or correlation integrals of the impulse response at two angles and bin positions as shown in figure 2.

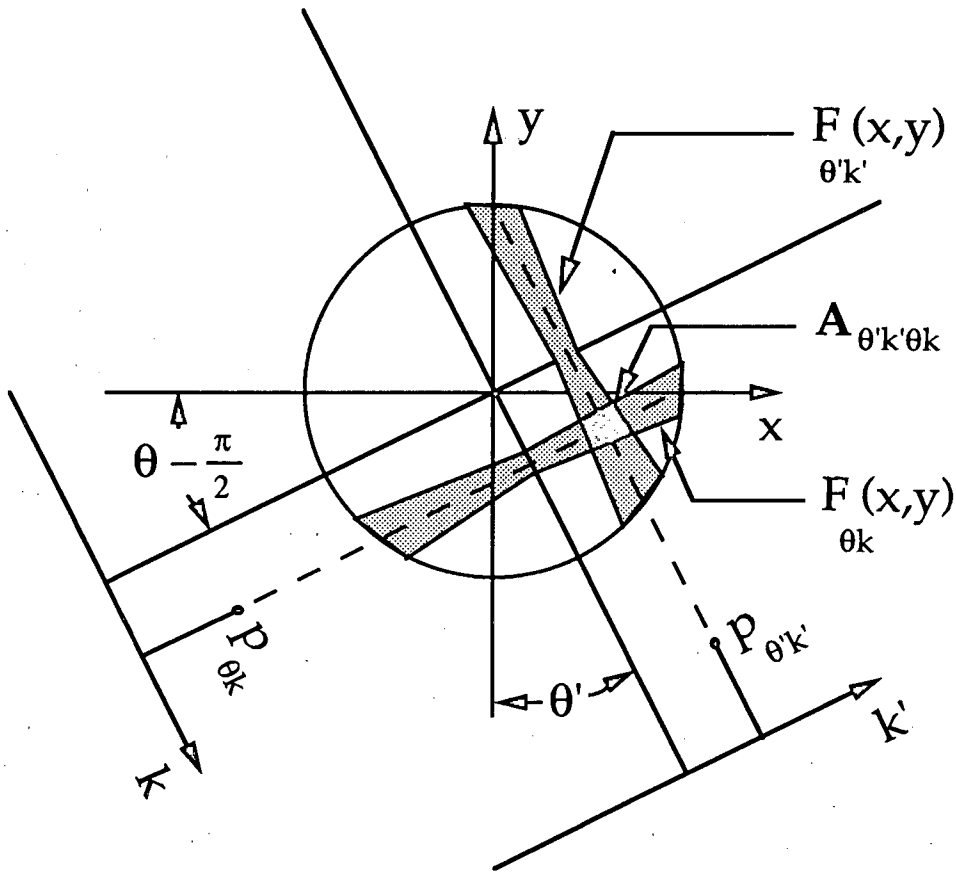


Figure 2: Schematic of projection normal matrix overlap integrals for two different angles and bin positions.

The SVD of  $A$  is given in equation 31. The singular values of  $A$  are asymptotically equal to the squares of the singular values of  $F$ ; therefore, by computing the smallest singular value of  $A$  we have found the desired error bound. The singular values of  $F$  are a function of the choice of the basis functional  $B_{ij}$ . The singular values of  $A$  are not a function of the basis functional but only of the projection functional; thus, we can compute its SVD without specifying the shape of pixels.

The computation of this SVD requires on the order of  $(m_\theta m_k)^3$  operations.<sup>[7],[2]</sup> For practical imaging systems, the product  $m_\theta m_k$  is approximately 60,000; thus, the computation of the SVD is usually computationally intractable. However, for a special class of rotationally invariant systems described in section 3, the computation problem is greatly simplified.

$$A = U_A S_A U_A^T. \quad (31)$$

### 2.3 System comparison

We have assumed that  $\bar{p}$  is the known variance of each projection measurement and  $F_{\theta k}$  has been predetermined. Now, we define the acceptable maximum variance in the reconstructed image to be  $\bar{b}$ . Thus, the minimum singular value of  $\mathbf{F}$  allowed in the computation of the pseudo-inverse  $\mathbf{F}^+$  to maintain the variance bound according to equation 28 is

$$S_{\min} = \sqrt{\frac{\bar{p}}{\bar{b}}}. \quad (32)$$

All singular values and the corresponding singular vectors less than  $S_{\min}$  should not be used. If  $N$  is the number of singular values greater than  $S_{\min}$ , then we should only reconstruct pixels that correspond to these  $N$  basis vectors of  $\mathbf{V}$ . In general, these  $N$  pixels are not the familiar square pixels used to display images.

We turn now the task of determining the number of angles,  $m_\theta$ , and bins,  $m_k$  needed with a fixed number of pixels,  $N$ , to obtain a desired maximum variance,  $\bar{b}$  in a reconstructed image. Again, assume that  $\bar{p}$  is the known variance of the projections and  $S_{\min}$  is as in equation 32. We must find a projection formation functional such that

$$S_{NN} = S_{\min}. \quad (33)$$

Since a closed form solution for the singular values of  $F_{\theta k}$  is not usually possible, this is done by computing the projection normal matrix and its SVD for various values of  $m_\theta$  and  $m_k$  until the desired value of  $S_{NN}$  is obtained.

## 3 ROTATIONAL INVARIANCE

When the elements of the projection normal matrix are a function of only the difference between  $\theta$  and  $\theta'$  modulo  $m_\theta$ , as shown in equation 34, the system is *rotationally invariant*. If it is not a function of the difference between  $k$  and  $k'$  modulo  $m_k$ , then the system is *radially variant*. When the system is rotationally invariant, the matrix can be written in block circulant form. The block circulant structure is shown in equation 37. There are  $m_\theta \times m_\theta$  blocks each of size  $m_k \times m_k$ .

$$A_{\theta'k'\theta k} = A_{[(\theta-\theta') \bmod m_\theta]k'0k} \quad (34)$$

$$= A_{[\Delta\theta \bmod m_\theta]k'0k} \quad (35)$$

$$= \int dy \int dx f_{[\Delta\theta \bmod m_\theta]k}(x, y) f_{0k}(x, y) \quad (36)$$

$$\mathbf{A} = \begin{bmatrix} A_0 & A_1 & A_2 & \dots & A_{m_\theta-2} & A_{m_\theta-1} \\ A_{m_\theta-1} & A_0 & A_1 & \dots & A_{m_\theta-3} & A_{m_\theta-2} \\ A_{m_\theta-2} & A_{m_\theta-1} & A_0 & \dots & A_{m_\theta-4} & A_{m_\theta-3} \\ \vdots & \vdots & \vdots & \ddots & \vdots & \vdots \\ A_2 & A_3 & A_4 & \dots & A_0 & A_1 \\ A_1 & A_2 & A_3 & \dots & A_{m_\theta-1} & A_0 \end{bmatrix} \quad (37)$$

Let  $f_k(x, y)$  denote the impulse response of a rotationally invariant, radially variant system, then equation 1 can be rewritten as

$$p_{\theta k} = \int dy \int dx f_k \left[ x \cos\left(\theta \frac{2\pi}{m_\theta}\right) + y \sin\left(\theta \frac{2\pi}{m_\theta}\right), -x \sin\left(\theta \frac{2\pi}{m_\theta}\right) + y \cos\left(\theta \frac{2\pi}{m_\theta}\right) \right] b(x, y). \quad (38)$$

$$A_{\theta'k'\theta k} = \int dy \int dx f_{k'} \left[ x \cos \left( \theta' \frac{2\pi}{m_{\theta'}} \right) + y \sin \left( \theta' \frac{2\pi}{m_{\theta'}} \right), -x \sin \left( \theta' \frac{2\pi}{m_{\theta'}} \right) + y \cos \left( \theta' \frac{2\pi}{m_{\theta'}} \right) \right] \quad (39)$$

$$f_k \left[ x \cos \left( \theta \frac{2\pi}{m_{\theta}} \right) + y \sin \left( \theta \frac{2\pi}{m_{\theta}} \right), -x \sin \left( \theta \frac{2\pi}{m_{\theta}} \right) + y \cos \left( \theta \frac{2\pi}{m_{\theta}} \right) \right] \quad (40)$$

$$= \int dy \int dx f_{k'} \left[ x \cos \left( \Delta\theta \frac{2\pi}{m_{\theta'}} \right) + y \sin \left( \Delta\theta \frac{2\pi}{m_{\theta'}} \right), -x \sin \left( \Delta\theta \frac{2\pi}{m_{\theta'}} \right) + y \cos \left( \Delta\theta \frac{2\pi}{m_{\theta'}} \right) \right] \quad (41)$$

$$f_k(x, y) \quad (42)$$

### 3.1 Block circulant singular value decomposition

An order  $m_k^2 m_{\theta} \log m_{\theta}$  fast Fourier transform (FFT) technique<sup>[9],[10]</sup> and an order  $m_{\theta} m_k^3$  SVD technique<sup>[7],[2]</sup> can be used to compute the block circulant singular value decomposition (BCSVD) of  $\mathbf{A}$  given in equation 43.<sup>[11]</sup> This represents asymptotic relative savings of  $m_{\theta}^2$  operations over a general SVD algorithm. The memory required is also reduced by a relative factor  $m_{\theta}$ .

$$\mathbf{A} = \mathbf{U}_A \mathbf{S}_A \mathbf{U}_A^T \quad (43)$$

$$= \mathbf{U}_A \mathbf{S}_D \mathbf{U}_A^T \quad (44)$$

$$= (\mathcal{F}_{m_{\theta}} \otimes \mathbf{I}_{m_k})^\dagger \mathbf{U}_D \mathbf{S}_D \mathbf{U}_D^\dagger (\mathcal{F}_{m_{\theta}} \otimes \mathbf{I}_{m_k}) \quad (45)$$

## 4 SUMMARY

The noise amplification characteristics of linear imaging systems can be analyzed by singular value decomposition (SVD). Analysis proceeds in three steps. First, the projection normal matrix is computed for a particular impulse response. The second step is to compute the SVD of the projection normal matrix. Finally, the singular values and consequently the imaging performance for different impulse response functions can be compared with the induced norm of the covariance of the estimated image used as a performance metric. This differs from deterministic approaches that use the ratio of the largest to smallest singular value (e.g., the condition number) as a metric. The maximum number of pixels possible for an acceptable noise level can be obtained for an existing system with a given number of angles and projection bins by computing the number of singular values greater than the square root of the ratio of projection variance and desired image variance. For the design of a new system, the number of angles and projection bins necessary to support a desired number of pixels can be computed by iteratively varying the number of angles and projection bins until the desired singular value spectra is obtained.

For a special class of rotationally invariant, radially variant systems that are quite common in practice, a fast parallel algorithm to compute the block circulant singular value decomposition (BCSVD) of the projection normal matrix can be used to make the analysis computationally feasible. This algorithm reduces computation time by a multiplicative factor equal to the number of equally spaced angles squared.

We are currently working on methods to extend the algorithm to weighted least squares and Poisson maximum likelihood estimators. Choosing the pixel basis functional such that is an eigenfunction of the right singular functions of the projection formation functional is also a topic of interest.

## 5 ACKNOWLEDGEMENTS

The authors would like to thank PG Coxson, SE Derenzo, RB Marr, MS Roos, and STS Wong for helpful discussions. This work was supported by the Office of Energy Research, Office of Health and Environmental Research, of the U.S. Department of Energy under contract No DE-AC03-76SF00098, by the National Institutes of Health, National Heart, Lung, and Blood Institute under grants No HL07367 and HL25840, National Institute of Aging under grant AG05890, by Cray Research Inc., and by IBM Inc.

## 6 REFERENCES

- [1] Lawson CL and RJ Hanson. *Solving Least Squares Problems*. Prentice-Hall, Englewood Cliffs, NJ, 1974.
- [2] Strang G. *Linear Algebra and Its Applications*. Academic Press, Orlando, FL, 1980.
- [3] Andrews HC and BC Hunt. *Digital Image Restoration*. Prentice-Hall, Englewood Cliffs, NJ, 1977.
- [4] Baker JR and TF Budinger. Advanced models for medical imaging. In *High Speed Computing: Scientific Applications and Algorithm Design*, pages 221–226, Urbana, IL, January 1987.
- [5] Huesman RH, EM Salmeron, and JR Baker. Compensation for crystal penetration in high resolution positron tomography. *IEEE Trans Nucl Sci*, **NS-36**:1100–1107, 1989.
- [6] Buonocore MH, WR Brody, and A Macovski. A natural pixel decomposition for two-dimensional image reconstruction. *IEEE Transactions on Biomedical Engineering*, **BME-28**(2):69–78, 1981.
- [7] Golub GH and C Reinsch. Singular value decomposition and least squares solutions. *Numer Math*, **14**:403–420, 1970.
- [8] Knuth DE. *The Art of Computer Programming*. Volume 2, Addison Wesley, Reading, MA, second edition, 1981.
- [9] Brigham EO. *The Fast Fourier Transform*. Prentice-Hall, Englewood Cliffs, NJ, 1974.
- [10] Bracewell RN. Fourier techniques in two dimensions. In Price JR, editor, *Fourier Techniques and Applications*, pages 45–71, Plenum Press, New York, 1985.
- [11] Baker JR. Macrotasking the singular value decomposition of block circulant matrices on the Cray-2. In *Proceedings of Supercomputing '89*, pages 243–247, Reno, NV, November 1989.

LAWRENCE BERKELEY LABORATORY  
TECHNICAL INFORMATION DEPARTMENT  
1 CYCLOTRON ROAD  
BERKELEY, CALIFORNIA 94720